HOKKAIDO UNIVERSITY

Title	Evaluation of Water Vapour Diffusion in Mchenga Sandstone
Author(s)	Yasidu, Umali Muhammad; Fujii, Yoshiaki; Kodama, Jun-ichi; Fukuda, Daisuke; Dandadzi, Johnson
Citation	MMIJ Fall Meeting 2017, 4(2), PY2-78
Issue Date	2017-09-26
Doc URL	http://hdl.handle.net/2115/67666
Type	proceedings
Note	MMIJ Fall Meeting 2017, Sept. 26-28 2017, Sapporo, Japan （資源・素材2017（札幌）：平成29年度資源・素材関係学協会合同秋季大会, 2017年9月26日～28日, 北海道大学, 札幌市）
File Information	PY2-78.pdf

Instructions for use

Hokkaido University Collection of Scholarly and Academic Papers : HUSCAP

若手ポスター発表（Poster：MMIJ Students and Young Researchers）
岩盤工学（ Rock Engineering）
Rock Engineering
2017年9月26日(火) 15:30 ～ 17:30 ポスター会場2 N301 (N棟3階/Fl.3.,Build. N)

[PY2-78] Evaluation of Water Vapour Diffusion in Mchenga Sandstone
Evaluation of Water Vapour Diffusion in Mchenga Sandstone

○Umali Muhammad YASIDU[1], Yoshiaki FUJII[1], Jun-ichi KODAMA[1], Daisuke FUKUDA[1], Johnson DANDADZI[2]
（1. Hokkaido University, 2. Mchenga Coal Mine）

キーワード：Coal Mines in Malawi, Roof falls, Vapour diffusion, Tensile strength

There are seven coalfields spread across Malawi, with four coalfields of bituminous coal located in the Northern Region where underground mining is done. One of the major challenges facing these coal mines is occurrence of hanging roof falls after the rainy season. It was clarified that the humidity was highest in April and May underground and that tensile strength of roof rocks decreased with environment humidity. To evaluate the extent of weakened zone around the roadways with time, water vapour diffusion in coal bearing rocks; arkose sandstone and fine-grained sandstone from Mchenga and Kaziwiziwi underground coal mines in the Livingstonia coalfield; was studied aiming to clarify the influencing factor of roof falls and to propose countermeasures against the roof falls. Rock samples from the mine were oven dried at 80˚C for seven days, jacketed using heat shrinkable tubing and oven dried again for three days. The specimens were then treated in high humidity achieved by pure water in isothermal condition (22˚C) in accordance with ASTM E96/E96M-16 water method. For comparison, Japanese Neogene tuffaceous Kimachi sandstone was also tested following the same procedure. The results of diffusion coefficient evaluations and numerical simulation will be shown.

©一般社団法人 資源・素材学会

1. Introduction

Moving from being an agro-based economy, Malawi has ventured into mining as its alternative economic driver towards the future. There are seven coalfields spread across the country, with four coalfields of bituminous coal in the Northern Region. Currently, four underground coal mining operations are running with additional two open pit mines in these coalfields. One of the major challenges facing these mines is occurrence of hanging roof falls during the rainy season. Potential roof falls in underground coal mines are one of the most significant hazards for miners. Roof falls can threaten miners, damage equipment, disrupt ventilation mechanisms and block installed emergency escape routes. For example, in the mine accidents recorded, on 1 November 2012, death of two miners and injury of other two was reported at Kaziwiziwi Coal Mine. In a previous study (Yasidu et al., 2017); the authors found that there were more severe accidents in May when the air humidity was the highest. In the study, the effect of humidity on strength of rocks in the underground coal mines in Malawi was clarified that the indirect tensile strength decreased with increase in humidity. Mchenga arkose sandstone indicated high sensitivity of 62% to humidity levels, a figure which was greater than sensitivity of Neogene tuffaceous Kimachi sandstone of Japan at 55.2%. This was attributed to clay mineral content of illite and zeolite in the rocks, respectively.

Chugh and Missavage (1981) studied the effect of moisture in strata control in coal mines. They summarised that moisture gain and moisture loss in mine rock is related to seasonal changes in absolute humidity of mine air. Water vapour from surrounding air of certain relative humidity enters the material or structure and is then transported by diffusion through the pore system of the material and adsorbed on the surface of the material (Keppert et al., 2016). In another research by Fujii et al. (2011) steel-arch removal test was carried out on a roadway at Kushiro Coal Mine, Japan in May, 2006. Initially, there was no large roof fall, even after 15 steel arches were removed. The unsupported span reached 16 m without large roof falls, except for rather small falls of loosened rocks that were as large as tens of centimeters. A few months later, in August and September, humid summer air flowed into the site and dripping water was seen on the rock surface. Then, several large rock falls, as large as 2 m occurred and it was estimated that the rock mass was weakened by the humid-air inflow and the large-scale roof falls were induced. It is likely that the roof rocks are weakened by the humid air and also fall in the mines in Malawi as the case study reveals. To investigate the extent of weakened zone of rocks around the roadways with time, the influencing factor for roof rock collapse and the countermeasures against the same more deeply, evaluation of diffusion coefficient and numerical simulation are required.

This paper describes the evaluation of water vapour diffusion coefficient in roof sandstone from Mchenga and Kaziwiziwi coal mines and results of basic simulations on the vapour migration into the roof rock.

2. Rock samples

Medium to coarse-grained arkose sandstone (arkose sandstone), ultra-fine to fine-grained sandstone (fine-grained sandstone) from Mchenga coal mine and Kaziwiziwi mine were used for the experiments. Mchenga coal mine (S10°42'55", E34°9'14") and Kaziwiziwi mine (S10°42'29", E34°9'50"), are located in the target area hosting the Livingstonia coalfield. The mines use room and pillar mining method. The pillar dimensions in Mchenga mine are 10 m x 10 m while in Kaziwiziwi mine measure 12 m x 12 m. The coal seam thickness ranges from 0.7 m to 3 m in Mchenga coal mine and 1.7 m to 2.3 m in Kaziwiziwi coal mine.

Stratigraphically, the area is composed of Karroo System strata (Permo-Carboniferous to Lower Jurassic) preserved in a number of N-S trending basins and down-faulted troughs that display faulted relationship to the underlying Precambrian to early Palaeozoic Basement Complex, mainly composed of paragneisses, granulites and felsic to ultramafic (meta-) igneous intrusive rocks. The basal beds of the succession consist of conglomerates and sandstones referred to the Dwyka (Carboniferous) and lower Ecca series (Permian). These are overlain by a sequence of carbonaceous shales and coal seams commonly called Coal Measures of lower Ecca series (Permian) (Cooper and Habgood, 1959). The roof stratum mainly consists of sandstone and shale of the upper Ecca group (Permian) (Figure 1).

From the analysis of the thin-sections, the Mchenga arkose sandstone showed a rich content of carbonate minerals and biotite. The matrix minerals included illite, cryptocrystalline siliceous minerals and carbonate minerals. On the other hand, the Mchenga fine-grained sandstone showed an argillaceous part lamination, a conspicuous black thick band. The matrix minerals included illite, goethite, coaly substances and opac minerals. Scanned images of the arkose sandstone showed no obvious open pore spaces (Figure 2). The surface exhibited a uniform colour and texture. As for the fine-grained sandstone, there were patches of different colours which could indicate different textures.

3. Method

Four sets of 10 cylindrical rock specimens (i.e. 40 specimens in total); measuring 30 mm in both length and diameter, were cut from blocks of the four types of rocks. The specimen ends were polished to a flatness of 0.02 mm.

Fig. 1 Rock samples from Mchenga coal mine (a) arkose sandstone (b) fine-grained sandstone; and Kaziwiziwi coal mine (c) arkose sandstone (d) fine-grained sandstone

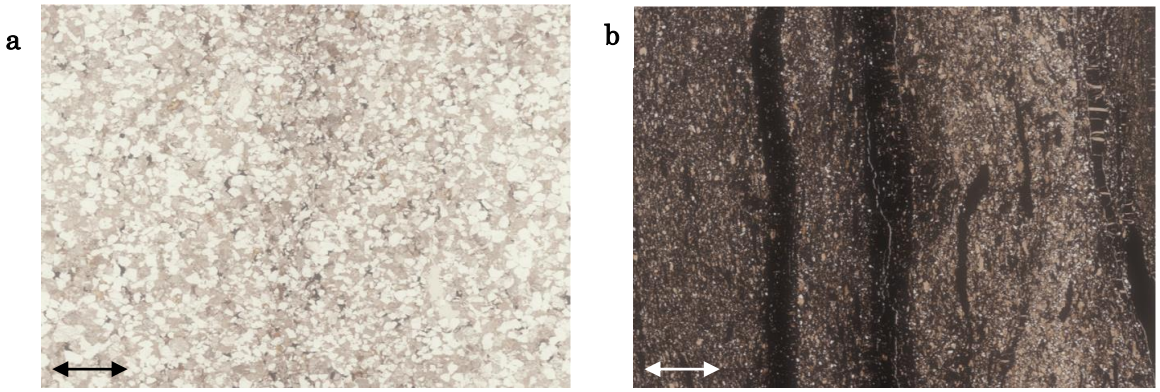

Fig. 2 Scanned images of specimens (a) Mchenga arkose sandstone (b) Mchenga fine-grained sandstone. The arrow length is 2mm.

3・1 Experimental setup

Specimens were oven dried at 80°C for a period of seven days. The dry specimens were jacketed with heat shrinkable tubing and were dried again in the oven at 80°C for another three days. After oven drying, dry weight of the specimens was measured using a balance with 1 mg resolution, and recorded.

Following that, the specimens were treated in high humidity (98%) achieved by pure/distilled water in accordance with the water method of ASTM E96/E96M-16. Subsequently, hourly measurements and recording of change in weight of the samples was carried out using a balance to determine the rate of water vapour movement through the specimen from the controlled atmosphere. Air-tight containers were used to maintain the applied humidity levels on the specimens (Figure 3).

This experiment setup was maintained in isothermal condition of 22°C in the laboratory for a period of 30 days.

Fig. 3 Jacketed samples in air-tight containers with pure water (a) arkose sandstone (b) fine-grained sandstone.

3・2 Evaluation

Vapour diffusion can be represented by Fick's law as:

$$\frac{\partial \theta}{\partial t} = D_v \frac{\partial^2 \theta}{\partial^2 x} \qquad (1)$$

where D_v ($m^2 \cdot s^{-1}$) is the diffusion coefficient, θ ($kg \cdot m^{-3}$) is the vapour density and x (m) is the distance along the longitudinal sample axis. Assuming θ_0 is applied at both ends of specimen at $t = 0$ and solving equation (1), the following equation is obtained:

$$\theta(\pi,t) = \theta_0 - \frac{4\theta_0}{\pi}\sum_{n=1}^{\infty}\frac{1}{2n-1}e^{-D_v\left(\frac{2n-1}{l}\pi\right)^2 t}\sin\frac{2n-1}{l}\pi x$$

Let Δm, A and l be the change in mass (kg), sectional area (m^2) and specimen length (m) respectively.

$$\Delta m = A\int_0^l \theta(x,t)\,\mathrm{d}x = A\int_0^l \theta_0\,\mathrm{d}x - A\frac{4\theta_0}{\pi}\sum_{n=1}^{\infty}\frac{1}{2n-1}e^{-D_v\left(\frac{2n-1}{l}\pi\right)^2 t}\int_0^l \sin\frac{2n-1}{l}\pi x\,\mathrm{d}x$$

$$= A\left[\theta_0 x\right]_0^l + A\frac{4\theta_0}{\pi}\sum_{n=1}^{\infty}\frac{1}{2n-1}\frac{l}{(2n-1)\pi}e^{-D_v\left(\frac{2n-1}{l}\pi\right)^2 t}\left[\cos\frac{2n-1}{l}\pi x\right]_0^l$$

$$= lA\theta_0 - A\frac{4\theta_0 l}{\pi^2}\sum_{n=1}^{\infty}\frac{1}{(2n-1)^2}e^{-D_v\left(\frac{2n-1}{l}\pi\right)^2 t}$$

Differentiating the equation with respect to time,

$$\frac{\partial \Delta m}{\partial t} \approx -\frac{4lA}{\pi^2}\theta_0\left\{-D_v\left(\frac{\pi}{l}\right)^2\right\}e^{-D_v\left(\frac{\pi}{l}\right)^2 t}$$

$$= 4lA\theta_0\frac{D_v}{l^2}e^{-D_v\left(\frac{\pi}{l}\right)^2 t}$$

Taking logarithm,

$$\ln\frac{\partial \Delta m}{\partial t} = \ln 4lA\theta_0\frac{D_v}{l^2} - D_v\left(\frac{\pi}{l}\right)^2 t$$

Letting α be the slope of $\ln \mathrm{d}(\mathrm{d}m/\mathrm{d}t) - t$ plot,

$$\alpha = -D_v\left(\frac{\pi}{l}\right)^2$$

$$\therefore\ D_v = -\alpha\left(\frac{l}{\pi}\right)^2 \qquad (2)$$

4. Results and Discussion

4・1 Mass change

Figures 4 and 5 show results of measurement of mass of specimens in this study. The mass increased rather rapidly in the initial stage and then almost converged. It was noted that arkose sandstone specimens generally had higher values of mass change as compared to other fine-grained sandstones for the Mchenga rocks.

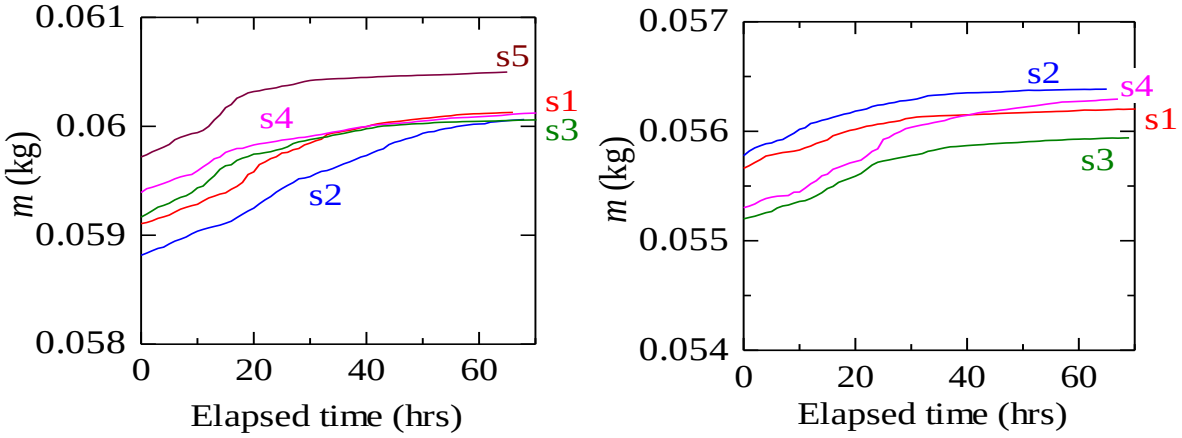

(a) **(b)**

Fig. 4 Mass variation against time for Mchenga rock samples (a) Mchenga arkose sandstone (b) Mchenga fine-grained sandstone.

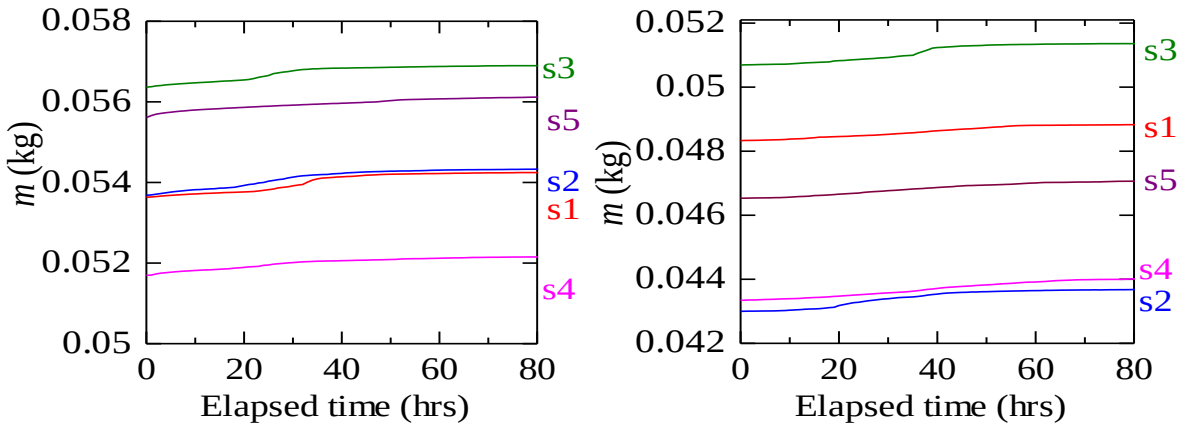

(a) **(b)**

Fig. 5 Mass variation against time for Kaziwiziwi rock samples (a) Kaziwiziwi arkose sandstone (b) Kaziwiziwi fine-grained sandstone.

4・2 Water vapour diffusion coefficients

Water vapour diffusion coefficient was calculated using equation (2). The gradient, α was calculated as the gradient of regression line from the ln d(dm/dt) -t graph ignoring the initial flat part. Average diffusion coefficient for Mchenga arkose sandstone was 1.02 x10^{-9} $m^2 \cdot s^{-1}$, while it was found to be 1.20 x 10^{-9} $m^2 \cdot s^{-1}$ for fine-grained sandstone (Figure 6). For Kaziwiziwi arkose sandstone and fine-grained sandstone, the average diffusion coefficients were 1.12 x 10^{-9} $m^2 \cdot s^{-1}$ and 0.60 x 10^{-9} $m^2 \cdot s^{-1}$ respectively (Figure 7). Diffusion coefficient value for sandstone is in the range of 1.60 x 10^{-6} $m^2 \cdot s^{-1}$ to 3.45 x 10^{-7} $m^2 \cdot s^{-1}$ (Keppert et al., 2016). The values of D_v from Malawi coal mines are smaller than the published results by orders of 2 and 3.

5. Vapour migration into the roof rocks

To get a better insight of the behaviour of the water vapour diffusion around the roadways in the underground coal mines, a numerical simulation of one-dimensional water vapour diffusion into a rock mass with sandstone was carried out using two-dimensional FE code. The FE code was originally built for heat analysis. However, replacing temperature and $\lambda/(\rho \cdot C)$; where λ, ρ and C are heat conductivity, density and specific heat respectively; by vapour density and D_v respectively, vapour diffusion can be calculated (equation (1) above).

A simple two-dimensional finite element mesh was generated, 0.1 m x 5 m (100 triangular elements, 102 nodes), as shown in Figure 8. The rock mass consisting of Mchenga arkose sandstone was assumed to be homogeneous, isotropic and completely dry at the initial condition. With water vapour diffusion coefficient D_v as 1.02 x 10^{-9} $m^2 \cdot s^{-1}$, and by setting density, ρ as 2,200 $kg \cdot m^{-3}$, λ as 0.0018 $J \cdot s^{-1} \cdot m^{-1} \cdot K^{-1}$ and C as 800 $J \cdot kg^{-1} \cdot K^{-1}$; a vapour density, θ_0 (10 $kg \cdot m^{-3}$) was applied at the lower boundary at time $t \geq 0$.

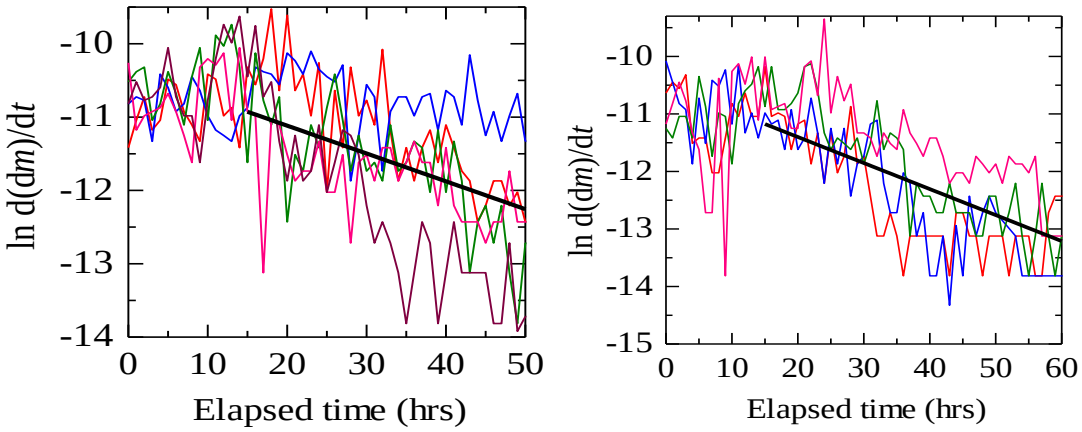

Fig. 6 Mass change of specimens as a function of elapsed time (a) Mchenga arkose sandstone (b) Mchenga fine-grained sandstone. The thick black line gives the average slope of the graphs to calculate average diffusion coefficient.

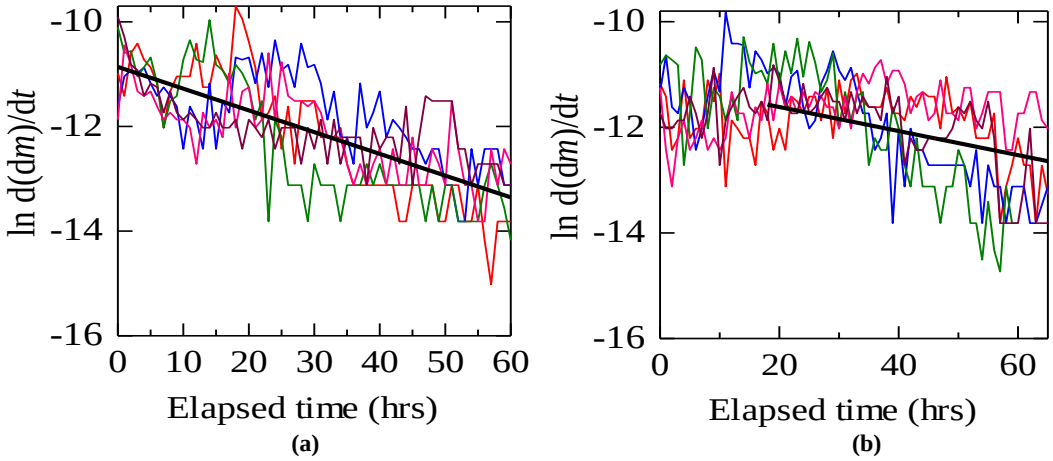

Fig. 7 Mass change of specimens as a function of elapsed time (a) Kaziwiziwi arkose sandstone (b) Kaziwiziwi fine-grained sandstone. The thick black line gives the average slope of the graphs to calculate average diffusion coefficient.

From the numerical model, delayed diffusion of water vapour into the dry roof rock was simulated (Figure 9). The difference between the peak humidity and peak accident occurrence may be explained by giving vapour density variation in the calculation for a longer period of time.

6. Conclusion

The water vapour diffusion coefficient of roof rocks from underground coal mines in Malawi was determined. Mchenga arkose sandstone had a diffusion coefficient of 1.02 x 10^{-9} $m^2 \cdot s^{-1}$ which is almost the same as that of fine-grained sandstone (1.20 x 10^{-9} $m^2 \cdot s^{-1}$). As for Kaziwiziwi rock samples, arkose sandstone had twice higher diffusion coefficient of 1.12 x 10^{-9} $m^2 \cdot s^{-1}$ than 0.60 x 10^{-9} $m^2 \cdot s^{-1}$ for fine-grained sandstone. It was confirmed that FEM for heat analysis can represent gradual water vapour migration into the rocks. Giving humidity variation in the calculation will explain the delay of peak accident occurrence from the highest humidity. Furthermore, 2-D analysis may explain the extent of weakened zones around a roadway in underground coal mines in future.

Acknowledgement

The authors appreciate Mchenga Coal Mine management, engineers and staff for their co-operation in conducting this study. This research is supported by JICA under KIZUNA Program (J-15-10275).

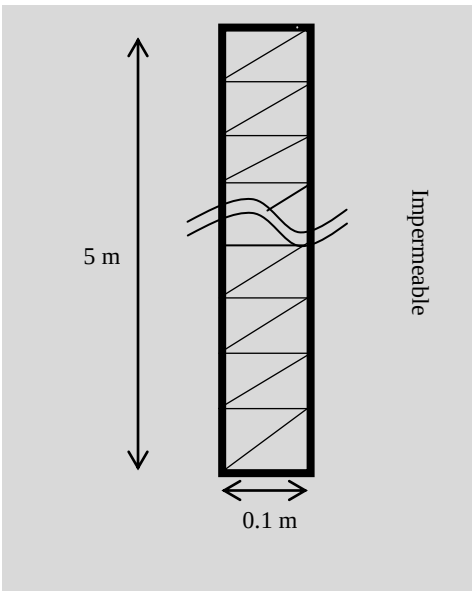

Fig. 8　Finite element mesh configuration used in numerical simulation. The top and side boundaries are insulated.

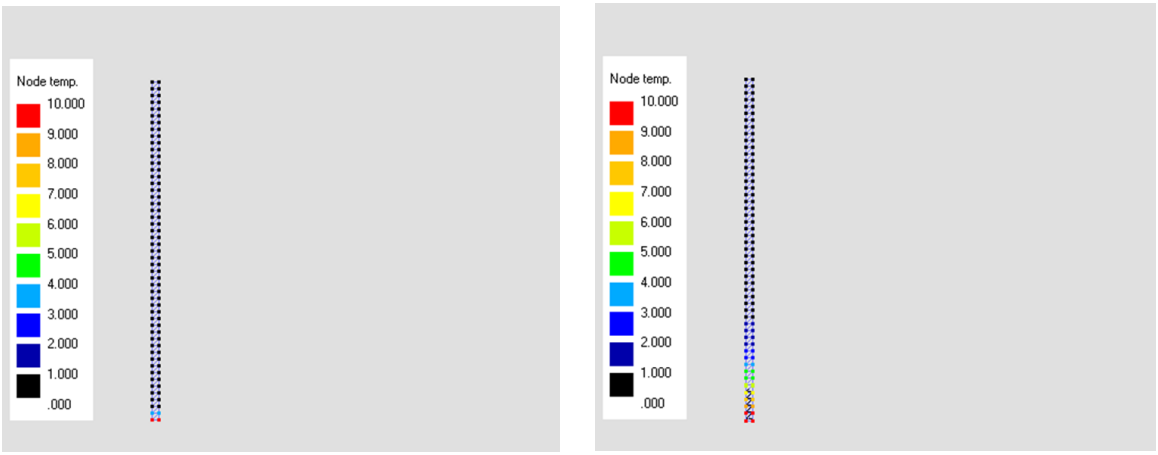

(a) 1 hour　　(b) 120 hours

Fig. 9　Simulated results of water vapour diffusion into dry roof rock: (a) after 1 hour (b) after 120 hours.

References

ASTM International, E96/E96M – 16. (2016), Standard Test Methods for Water Vapor Transmission of Materials, ASTM Int. Standards, pp. 4-6.

Chugh, Y.P. and R.A. Missavage. (1981), Effects of Moisture on Strata Control in Coal Mines. Eng. Geol., 17: 241--255.

Cooper, G.G.W. and F. Habgood. (1959), The Geology of Livingstonia Coalfield, Nyasaland Geological Survey Department Bulletin No. 11, Zomba, Government Printer.

Fujii, Y., Y. Ishijima, Y. Ichihara, T. Kiyama, S. Kumakura, M. Takada, T. Sugawara, T. Narita, J. Kodama, M. Sawada, and E. Nakata. (2011), Mechanical Properties of Abandoned and Closed Roadways in the Kushiro Coal Mine, Japan. Int. J. of Rock Mech. & Min. Sci. 48: 585–596.

Keppert, M., J. Zumar, M. Cachova, D. Konakova, P. Svora, Z. Pavlik, E. Vejmelkova, and R. Cerny. (2016), Water Vapor Diffusion and Adsorption of Sandstones: Influence of Rock Texture and Composition. Advances in Materials Sci. and Eng. 2016: ID 8039748.

Yasidu, U., Y. Fujii, J. Kodama and D. Fukuda. (2017), Effect of Humidity on Strength of Rocks in Underground Coal Mines in Malawi. Proceedings of 52nd U.S. Symp. on Rock Mech. / Geomech, San Francisco.